Distance-Based Topological Indices of Nanosheets, Nanotubes, and Nanotori of SiO_2

Micheal Arockiaraj[a], Sandi Klavžar[b,c,d], Shagufa Mushtaq[a,*], Krishnan Balasubramanian[e]

[a]Department of Mathematics, Loyola College, Chennai 600034, India

[b]Faculty of Mathematics and Physics, University of Ljubljana, Slovenia

[c]Faculty of Natural Sciences and Mathematics, University of Maribor, Slovenia

[d]Institute of Mathematics, Physics and Mechanics, Ljubljana, Slovenia

[e]School of Molecular Sciences, Arizona State University, Tempe AZ 85287-1604, USA

Abstract

We have computed distance-based topological indices of nanosheets, nanotubes and nanotori of SiO_2 which find potential applications in drug, food, and cosmetic industry. As topological indices correlate with physico-chemical properties and estimating efficiency of drug deliveries of these species, we compute the topological indices based on their degrees and distances of the associated molecular graphs. We have obtained exact analytical expressions of various topological indices such as the Wiener, vertex-Szeged, edge-Szeged, edge-vertex Szeged, Padmakar-Ivan, Schultz and Gutman indices of SiO_2 nanosheet, nanotube and torus using the cut method which involves decomposing a molecular graph by means of the transitive closure property of Djoković-Winkler relation to smaller strength-weighted quotient graphs.

Keywords: Silicon dioxide nanostructures, drug delivery, QSAR/QSPR, cut method, topological indices.

1 Introduction

Graph theory finds numerous applications in several areas of chemistry such as quantitative structure-activity relations, topological characterization of chemical structures, prediction of biological activities, quantum chemistry, proteomics, spectroscopy, isomer enumeration, graph polynomials for

*Corresponding author : shagufamushtaq95@gmail.com

structural characterizations, nuclear spin statistics, NMR spectroscopy, statistical and other methods for prediction of toxicity, structure-property relations of fullerenes, mesoporous materials, nanomaterials and so on [3–5, 7–9, 11–15, 17, 18, 47, 52, 53].

Quantitative structure activity and property relationships (QSAR/QSPR) make use of the relation between the molecular connectivity of chemical compounds and their properties and thus the underlying graph-theoretical properties constitute the basis for computer-aided drug discovery and predictive toxicology. Consequently, successful uses of quantitative structure-activity and property relationships have stimulated the emergence of various topological descriptors of molecules, periodic structures, fullerenes, lattices, proteomes and nanomaterials [8, 9, 11–15, 17, 18, 20, 32, 47–49, 53, 63]. The basic mathematical techniques of graph reductions, iterative methods, recursive methods, tree-pruning algorithms etc., have been applied to the derivations of a number of topological properties such as spectral polynomials, matching polynomials, distance polynomials of chemical structures, fullerenes, organic polymers, nanotubes and lattices of varied complexity as seen from refs. [6, 9, 10, 12, 13, 15]. The nature of intermolecular interactions depends on the degree and distance parameters, and moreover a number of physico-chemical properties of compounds such as boiling points, melting points, vapor pressures, dermal penetration, octanol partition coefficients, chromatographic retention indices, 2D-gel electrophoresis patterns of proteomes [14] etc., have been shown to correlate with topological properties as good starting points. Although one may need more sophisticated quantum chemical and biodescriptors as well as quantum molecular dynamics simulations for more accurate predictions of chemical and biological properties, due to computationally intensive nature of such methods, topological methods have found useful applications due to relative ease with which they can be computed.

Wiener index [62] which is a distance-based topological descriptor has been studied over the years since it is readily computed and it appears to correlate with many physico-chemical properties of organic compounds and has found to have applications in other fields such as crystallography, communication theory, facility location, ornithology [16], and so on [42, 56]. In fact as shown in [16], interaction between a flock of birds depends more intimately on the topological distance rather than the Euclidian distance. Hence there are properties that depend more on topological relation than geometric relation. Since the advent of Wiener index several other topological indices have been formulated such as the Schultz index [57], Gutman index [29], hyper-Wiener [55], edge-Wiener [44], vertex-edge Wiener [44], vertex-Szeged [29], edge-Szeged [30], edge-vertex Szeged [43], total Szeged [46], PI index [35], Randić index [54], Zagreb indices [31], ABC [24], harmonic [25], geometric-arithmetic [60], sum-connectivity index [64], and so on.

Silicon dioxide, one of the most important materials, finds wide-ranging applications in semiconductor industry to biology. It is widely used as an absorbent, anti-caking agent and in drugs as an inactive filler. Silica based nanomaterials have attracted considerable attention in recent years due to their tunable particle size and specific surface area, abundant Si-OH bonds on the particle surface that lend to functionalization [52], chemical/thermal stability, high drug loading capability, and sustained drug release thereby enhancing bioavailability of drugs [21, 33, 50, 59, 65]. In order to study the utilization of silica nanoparticles in pharmaceutical industry, the study of QSAR/QSPR properties is of paramount importance for determining the efficacy and toxicity of these compounds. In recent years functionalized mesoporous silicate based nanomaterials have found applications in a number of areas ranging from efficient drug delivery, nanomedicine to sequestration of high-level nuclear materials [21, 33, 50, 52, 59, 65]. Many properties such as toxicity, dermal penetrations, guest-host interactions, protein-drug interactions, receptor binding propensity, drug metabolomics, etc., depend on the structural parameters, pore sizes, intermolecular interactions, electronic and electrostatic properties many of which depend on the underlying topological distances and thus topological indices are attractive starting points to any statistical approach for obtaining structure-activity relations. In this paper, we have computed topological indices for SiO_2 nanosheets and then we proceed to form nanotubes and nanotori from these sheets in order to compute various topological indices for such newly formulated structures.

In the following section we recall graph-theoretical terminology needed and define the distance-based topological indices of interest. In Section 3 we develop the computational techniques to be applied and derive a new theoretical result that allows their implementation. In Section 4 we proceed to compute the topological indices of various SiO_2 nanostructures and discuss the asymptotic behaviors for the analytical expressions obtained based on the large values of their parameters along with a comparative analysis of the indices. The key tool for these computations is the so-called cut method that was first introduced in [38] for the situation when cuts coincide with the Θ-classes of a given graph and the topological index considered is the classical Wiener index. Later the method was extended to arbitrary graphs where cuts are Θ^*-classes [36]. Numerous papers followed in which the cut method was developed for other distance-based (and also some not distance-based) topological indices of families of (chemical) graph. For a survey on the cut method see [42].

2 Graph-theoretical terminology and distance-based indices

Throughout this paper, we consider only simple and finite connected graphs. If $G = (V(G), E(G))$ is a graph, then $d_G(u, v)$ denotes the usual shortest-path distance between the vertices $u, v \in V(G)$, that is, the number of edges on a shortest u, v-path. The shortest distance between the vertex u and the edge $f = xy \in E(G)$ is defined as $d_G(u, f) = min\{d_G(u, x), d_G(u, y)\}$. The degree of a vertex v is denoted with $d_G(v)$, and the open neighborhood $N_G(v)$ is the set of vertices adjacent to v. For an edge $e = uv \in E(G)$, the following sets will be utmost important:

$$\begin{aligned} N_u(e|G) &= \{x \in V(G) : \; d_G(u, x) < d_G(v, x)\}\,, \\ M_u(e|G) &= \{f \in E(G) : \; d_G(u, f) < d_G(v, f)\}\,. \end{aligned}$$

The cardinality of $N_u(e|G)$ and $M_u(e|G)$ is denoted by $n_u(e|G)$ and $m_u(e|G)$ respectively. The quantities $n_v(e|G)$ and $m_v(e|G)$ are defined analogously. Using these notations we collect in Table 1 the definitions of relevant distance-based topological indices.

Table 1: Topological indices of a simple graph G

Topological indices	**Mathematical expressions**
Wiener [61]	$W(G) = \sum_{\{u,v\}\subseteq V(G)} d_G(u, v)$
Vertex-Szeged [29]	$Sz_v(G) = \sum_{e=uv\in E(G)} n_u(e\|G)n_v(e\|G)$
Edge-Szeged [30]	$Sz_e(G) = \sum_{e=uv\in E(G)} m_u(e\|G)m_v(e\|G)$
Edge-vertex-Szeged [43]	$Sz_{ev}(G) = \frac{1}{2} \sum_{e=uv\in E(G)} \Big[n_u(e\|G)m_v(e\|G) + n_v(e\|G)m_u(e\|G)\Big]$
Total-Szeged [46]	$Sz_t(G) = Sz_v(G) + Sz_e(G) + 2Sz_{ev}(G)$
Padmakar-Ivan [35]	$PI(G) = \sum_{e=uv\in E(G)} \Big[m_u(e\|G) + m_v(e\|G)\Big]$
Schultz [57]	$S(G) = \sum_{\{u,v\}\subseteq V(G)} \Big[d_G(u) + d_G(v)\Big] d_G(u, v)$
Gutman [29]	$Gut(G) = \sum_{\{u,v\}\subseteq V(G)} d_G(u)d_G(v)d_G(u, v)$

The concept of a *strength-weighted graph* was introduced in [2] as a triple $G_{sw} = (G, SW_V, SW_E)$, where

- G is a graph,
- SW_V is the set of ordered pairs (w_v, s_v), $v \in V(G)$, with w_v being the vertex-weight and s_v the vertex-strength of v, and
- SW_E is the set of ordered pairs (w_e, s_e), $e \in E(G)$, with w_e being the edge-weight and s_e the edge-strength of e.

In this paper we restrict to the case $w_e = 1$ for every edge. From now on the strength-weighted graph will be $G_{sw} = \big(G, (w_v, s_v), s_e\big)$. For any vertex $u \in G_{sw}$, the open neighborhood of u is given as $N_{G_{sw}}(u) = N_G(u)$ and the degree of the vertex u as $d_{G_{sw}}(u) = 2s_v(u) + \sum\limits_{x \in N_{G_{sw}}(u)} s_e(ux)$. Also, for an edge $uv \in G_{sw}$ we set

$$\begin{aligned} n_u(e|G_{sw}) &= \sum_{x \in N_u(e|G_{sw})} w_v(x), \\ m_u(e|G_{sw}) &= \sum_{x \in N_u(e|G_{sw})} s_v(x) + \sum_{f \in M_u(e|G_{sw})} s_e(f). \end{aligned}$$

Analogously, we define the terms $n_v(e|G_{sw})$ and $m_v(e|G_{sw})$. In Table 2 we present the topological indices for strength-weighted graphs as introduced in [2].

If TI denotes an arbitrary topological index discussed in the paper, then for $w_v = s_e = 1$ and $s_v = 0$ we have $TI(G_{sw}) = TI(G)$. The *weighted-Wiener index* that was introduced in [37] (see also [41]) is the particular case of the strength-weighted graph for $s_v = 0$ and $s_e = 1$, while the vertex, edge, and edge-vertex versions of the Szeged index and the PI index were considered using vertex-edge weighted graphs in [22, 58].

3 Computational techniques

In this section we first outline the preliminaries and basic concepts needed to develop the cut method. Then theorems that express distance-based indices of strength-weighted graphs using the cut method are presented. The section is concluded with a classification of Θ^*-classes in subdivision graphs of partial cubes, a key step for the investigation of the SiO_2 nanostructures later on.

A subgraph H of a graph G is *isometric* if $d_H(u, v) = d_G(u, v)$ holds for all $u, v \in V(H)$. If H and G are disjoint graphs, then a mapping $f : V(H) \to V(G)$ is an *isometric embedding* if $f(H)$ is

Table 2: Topological indices for strength-weighted graph G_{sw}

Topological index	Mathematical expressions
Wiener	$W(G_{sw}) = \sum_{\{u,v\}\subseteq V(G_{sw})} w_v(u)w_v(v)d_{G_{sw}}(u,v)$
Vertex-Szeged	$Sz_v(G_{sw}) = \sum_{e=uv\in E(G_{sw})} s_e(e)n_u(e\|G_{sw})n_v(e\|G_{sw})$
Edge-Szeged	$Sz_e(G_{sw}) = \sum_{e=uv\in E(G_{sw})} s_e(e)m_u(e\|G_{sw})m_v(e\|G_{sw})$
Edge-vertex-Szeged	$Sz_{ev}(G_{sw}) = \frac{1}{2}\sum_{e=uv\in E(G_{sw})} s_e(e)\Big[n_u(e\|G_{sw})m_v(e\|G_{sw})+ n_v(e\|G_{sw})m_u(e\|G_{sw})\Big]$
Total-Szeged	$Sz_t(G_{sw}) = Sz_v(G_{sw}) + Sz_e(G_{sw}) + 2Sz_{ev}(G_{sw})$
Padmakar-Ivan	$PI(G_{sw}) = \sum_{e=uv\in E(G_{sw})} s_e(e)\Big[m_u(e\|G_{sw}) + m_v(e\|G_{sw})\Big]$
Schultz	$S(G_{sw}) = \sum_{\{u,v\}\subseteq V(G_{sw})} \Big[w_v(v)d_{G_{sw}}(u) + w_v(u)d_{G_{sw}}(v)\Big]d_{G_{sw}}(u,v)$
Gutman	$Gut(G_{sw}) = \sum_{\{u,v\}\subseteq V(G_{sw})} d_{G_{sw}}(u)d_{G_{sw}}(v)d_{G_{sw}}(u,v)$

an isometric subgraph of G. A subgraph H of a graph G is *convex* if for every $u, v \in V(G)$, every shortest u, v-path in H lies completely in G. The *Djoković-Winkler relation* Θ (due to [23, 62]) is defined on $E(G)$ as follows: if $e = ab \in E(G)$ and $f = cd \in E(G)$, then $e\Theta f$ if $d_G(a, c) + d_G(b, d) \neq d_G(a, d) + d_G(b, c)$. The relation Θ is reflexive and symmetric, but in general not transitive. Its transitive closure Θ^* hence forms an equivalence relation on $E(G)$ and partitions $E(G)$ into Θ^*-classes $\mathcal{F}(G) = \{F_1, \ldots, F_r\}$. Let G/F_i, $1 \leq i \leq r$, be the *quotient graph* w.r.t. Θ^*, that is, the graph whose vertices are the connected components of the graph $G - F_i$, two components C and D being adjacent if there exists an edge $uv \in F_i$ such that $u \in C$ and $v \in D$.

A partition $\mathcal{E}(G) = \{E_1, \ldots, E_k\}$ of $E(G)$ is said to be *coarser* than the partition $\mathcal{F}(G)$, if each set E_i is the union of one or more Θ^*-classes of G. Vertices $x, y \in V(G)$ are in *relation* R if $N_G(x) = N_G(y)$. The relation R is an equivalence relation, and thus the R-equivalence class of $x \in V(G)$ will be denoted $[x]_R$. (We note that using relation R the Wiener index of a weighted graph from [41] was furthermore reduced in [40].) We can now state the following key theorems for the rest of the paper.

Theorem 1. [2] *Let* $G_{sw} = \big(G, (w_v, s_v), s_e\big)$ *be a strength-weighted graph and let* $\mathcal{E}(G_{sw}) = \{E_1, \ldots, E_k\}$ *be a partition of* $E(G)$ *coarser than* $\mathcal{F}(G_{sw})$*. If* $TI \in \{W, Sz_v, Sz_e, Sz_{ev}, PI, S, Gut\}$*, then*

$$TI(G_{sw}) = \sum_{i=1}^{k} TI(G/E_i, (w_v^i, s_v^i), s_e^i)\,,$$

where

- $w_v^i : V(G/E_i) \to \mathbb{R}^+$ *is defined by* $w_v^i(C) = \sum_{x \in C} w_v(x)$*,* $\forall\ C \in G/E_i$*,*
- $s_v^i : V(G/E_i) \to \mathbb{R}^+$ *is defined by* $s_v^i(C) = \sum_{xy \in C} s_e(xy) + \sum_{x \in C} s_v(x)$*,* $\forall\ C \in G/E_i$*,*
- $s_e^i : E(G/E_i) \to \mathbb{R}^+$ *is defined by* $s_e^i(CD) = \sum_{\substack{xy \in E_i \\ x \in C, y \in D}} s_e(xy)$*, for any* $C, D \in V(G/E_i)$*.*

Theorem 2. [2] *Let* $G_{sw} = \big(G, (w_v, s_v), s_e\big)$ *be a strength-weighted graph such that* $a \in V(G_{sw})$ *and* $A = [a]_R$*. Let* $G_{sw}^{'} = \big(G^{'}, (w_v^{'}, s_v^{'}), s_e^{'}\big)$ *be defined with* $G^{'} = G - (A - \{a\})$*,* $w_v^{'}(a) = \sum_{x \in A} w_v(x)$*,* $s_v^{'}(a) = \sum_{x \in A} s_v(x)$*, for any* $b \in N_{G_{sw}^{'}}(a)$*,* $s_e^{'}(ab) = \sum_{x \in A} s_e(xb)$ *and* $w_v^{'}(x) = w_v(x)$*,* $s_v^{'}(x) = s_v(x)$*,* $s_e^{'}(xy) = s_e(xy)$*, for any* $x \notin A$*,* $y \notin A$*. Then*

(i) $W(G_{sw}) = W(G_{sw}^{'}) + \sum_{\{x,y\} \in \binom{A}{2}} 2w_v(x)w_v(y)$,

(ii) $S(G_{sw}) = S(G_{sw}^{'}) + \sum_{\{x,y\} \in \binom{A}{2}} 2\Big(w_v(y)d_{G_{sw}}(x) + w_v(x)d_{G_{sw}}(y)\Big)$,

(iii) $Gut(G_{sw}) = Gut(G_{sw}^{'}) + \sum_{\{x,y\} \in \binom{A}{2}} 2d_{G_{sw}}(x)d_{G_{sw}}(y)$.

Recall that the hypercube Q_n, $n \geq 1$, has all binary strings of length n as vertices, two vertices being adjacent if they differ in precisely one coordinate. A connected graph G is said to be a *partial cube* if there exists $n \geq 1$ and an isometric embedding $f : V(G) \to V(Q_n)$. It is well-known that G is a partial cube if and only if G is bipartite and $\Theta = \Theta^*$. In other words, partial cubes are precisely bipartite graphs with transitive relation Θ [62]. The Θ-equivalence classes of a partial cube G are (also) called cuts. Many important classes of chemical graphs are partial cubes as for instance trees, phenylenes, and benzenoid systems.

If G is a graph, then the *subdivision graph* $Sub(G)$ of G is the graph obtained from G by replacing every edge uv of G with a new vertex x_{uv} and connecting x_{uv} with u and v.

Theorem 3. *Let $\mathcal{F}(G) = \{F_1, \ldots, F_r\}$ be the Θ-partition of a partial cube G. Then the Θ^*-partition $\mathcal{F}'(Sub(G))$ of the subdivision graph $Sub(G)$ contains the following classes arising from F_i, $1 \le i \le r$:*

- *If $F_i = \{uv\}$, then $\{ux_{uv}\} \in \mathcal{F}'(Sub(G))$ and $\{vx_{uv}\} \in \mathcal{F}'(Sub(G))$;*
- *If $F_i = \{uv, u'v'\}$, then $\{ux_{uv}, v'x_{u'v'}\} \in \mathcal{F}'(Sub(G))$ and $\{vx_{uv}, u'x_{u'v'}\} \in \mathcal{F}'(Sub(G))$;*
- *If $F_i = \{u_1v_1, \ldots, u_kv_k\}$, $k \ge 3$, then $\{u_1x_{u_1v_1}, v_1x_{u_1v_1}, \ldots, u_kx_{u_kv_k}, v_kx_{u_kv_k}\} \in \mathcal{F}'(Sub(G))$.*

Proof. It is well-known that $|F_i| = 1$ if and only if the edge $e \in F_i$ is a bridge. Hence in $Sub(G)$ the edge $e = uv \in E(G)$ leads to two bridges of $Sub(G)$ which are then Θ^*-classes of $Sub(G)$. In the rest of the proof we may assume that $|F_i| \ge 2$.

Let $uv \in F_i$ and let $ab \in E(G)$, where $a, b \in N_u(e|G)$. Since G is bipartite, there exists an integer t such that $d_G(u, a) = t$ and $d_G(u, b) = t + 1$. Moreover, since G is a partial cube, we also have $d_G(v, a) = t + 1$ and $d_G(v, b) = t + 2$. In $Sub(G)$, the distance between any pair of different vertices from $\{u, v, a, b\}$ is twice the distance between the same vertices in G, hence in $Sub(G)$ there exists a shortest path of the following form:

$$v \to x_{uv} \to u \to \cdots \to a \to x_{ab} \to b\,.$$

As no edges of a shortest path are in relation Θ, it follows that no two different edges from $\{ux_{uv}, vx_{uv}, ax_{ab}, bx_{ab}\}$ are in relation Θ in $Sub(G)$. Consequently, none of the edges ux_{uv} and vx_{uv} is in relation Θ with any of the edges in $Sub(G)$ arising from the edges in $N_u(e|G)$. Analogously, none of the edges ux_{uv} and vx_{uv} is in relation Θ with any of the edges in $Sub(G)$ arising from the edges in $N_v(e|G)$. In conclusion, ux_{uv} and vx_{uv} can only be in relation Θ with edges of the form $u'x_{u'v'}$ and $v'x_{u'v'}$, where $u'v' \in F_i$.

Suppose now that $F_i = \{uv, u'v'\}$. Then, clearly, $ux_{uv}\Theta v'x_{u'v'}$ and $vx_{uv}\Theta u'x_{u'v'}$. By the above we conclude that $\{ux_{uv}, v'x_{u'v'}\}$ and $\{vx_{uv}, u'x_{u'v'}\} \in \mathcal{F}'(Sub(G))$.

Assume finally that $F_i = \{u_1v_1, \ldots, u_kv_k\}$, where $k \ge 3$. Then $u_1x_{u_1v_1}\Theta v_2x_{u_2v_2}$, $u_1x_{u_1v_1}\Theta v_3x_{u_3v_3}$, …, $u_1x_{u_1v_1}\Theta v_kx_{u_kv_k}$. As similar conclusion holds for any edge $u_ix_{u_iv_i}$ as well as for $v_iu_1x_{u_iv_i}$, using the transitivity it follows that the Θ^*-class containing $u_1x_{u_1v_1}$ contains all the edges $u_1x_{u_1v_1}$, $v_1x_{u_1v_1}$, …, $u_kx_{u_kv_k}$, $v_kx_{u_kv_k}$. Moreover, by the above this class contains no other edge and we are done. □

In view of Theorem 3 we note that it was proven in [39] that for a connected graph G its subdivision graph is a partial cube if and only if every block of G is either a cycle or a complete graph.

If G is not a partial cube, then determining Θ^*-classes of $Sub(G)$ from the Θ^*-classes of G seems to be more involved. For instance, the complete graph K_n, $n \geq 1$, has a single Θ^*-class, that is, $\mathcal{F}(K_n) = \{E(K_n)\}$. By the above theorem from [39] we know that $Sub(K_n)$ is a partial cube. Moreover, it contains n Θ-classes. This example shows that even in the class of graphs G for which if $|\mathcal{F}(G)| = 1$ holds, the value $|\mathcal{F}(Sub(G))|$ is not bounded. A simpler example demonstrating the same fact is the following: Let C_{2n+1} represent the odd cycle of $2n+1$ vertices. Then $\mathcal{F}(C_{2n+1}) = \{E(C_{2n+1})\}$ and $|\mathcal{F}(Sub(C_{2n+1}))| = 2n+1$.

4 SiO_2 nanostructures

Silicon dioxide (SiO_2) consists of a giant covalent structure in which each silicon atom is covalently bonded to four oxygen atoms and each oxygen atom is covalently bonded to two silicon atoms as depicted in Fig. 1. Since the ratio is two oxygen atoms to each silicon atom, the formula is

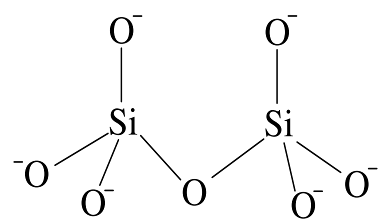

Figure 1: A silicon dioxide

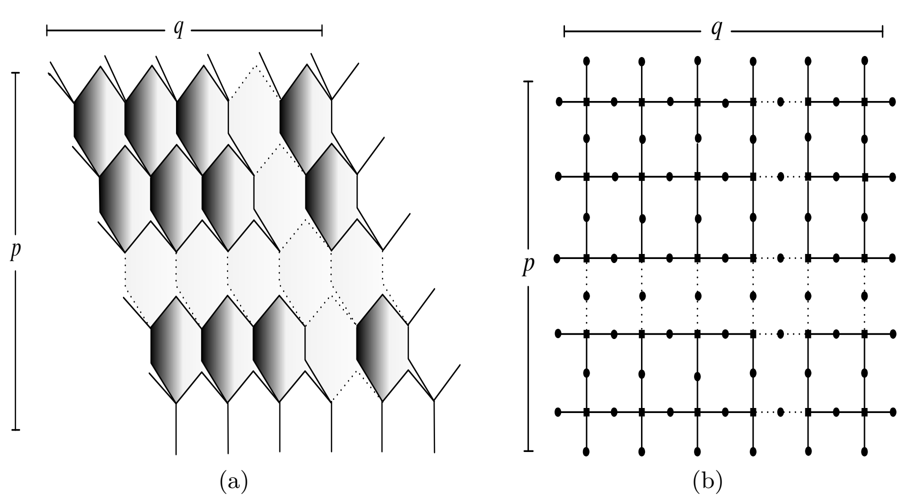

Figure 2: $SiO_2(p, q)$ layer structure (a) Original form (b) Bricks form

given as SiO_2. The molecular structure of silicon dioxide forms an octagon structure and when these octagons are joined together they form an SiO_2 layer structure as shown in Fig. 2(a). For convenience, we consider the isomorphic structure of SiO_2 layer structure as shown in Fig. 2(b) for efficient computation of topological indices by applying the cut method. The number of rows are represented by p and the number of columns by q which are the length and width of the nanosheet respectively, the structure in Fig. 2 is of dimension (p, q). Various degree-based topological indices of SiO_2 layer structure have been computed in [19, 26–28]. We now proceed to obtain the distance-based topological indices for different classes of SiO_2 nanostructures.

4.1 Topological indices of SiO_2 layer structure

In this section, we compute the distance-based indices of SiO_2 layer structure.

Theorem 4. *Let G be an SiO_2 layer structure of dimension (p, q), $p, q \geq 1$.*

1. $W(G) = \frac{1}{3}\big[9(p^3q^2 + p^2q^3) + 24(p^3q + pq^3) + 72p^2q^2 + 16(p^3 + q^3) + 141(p^2q + pq^2) + 84(p^2 + q^2) + 228pq + 116(p + q) + 48\big]$,

2. $SZ_v(G) = \frac{1}{3}\big[18p^3q^3 + 69(p^3q^2 + p^2q^3) + 67(p^3q + pq^3) + 258p^2q^2 + 16(p^3 + q^3) + 273(p^2q + pq^2) + 84(p^2 + q^2) + 322pq + 116(p + q) + 48\big]$,

3. $SZ_e(G) = \frac{2}{3}\big[16p^3q^3 + 42(p^3q^2 + p^2q^3) + 34(p^3q + pq^3) + 108p^2q^2 + 8(p^3 + q^3) + 87(p^2q + pq^2) + 18(p^2 + q^2) + 66pq + 10(p + q)\big]$,

4. $SZ_{ev}(G) = \frac{1}{6}\big[48p^3q^3 + 155(p^3q^2 + p^2q^3) + 133(p^3q + pq^3) + 492p^2q^2 + 32(p^3 + q^3) + 451(p^2q + pq^2) + 120(p^2 + q^2) + 442pq + 124(p + q) + 36\big]$,

5. $SZ_t(G) = \frac{2}{3}\big[49p^3q^3 + 154(p^3q^2 + p^2q^3) + 134(p^3q + pq^3) + 483p^2q^2 + 32(p^3 + q^3) + 449(p^2q + pq^2) + 120(p^2 + q^2) + 448pq + 130(p + q) + 42\big]$,

6. $PI(G) = 16p^2q^2 + 22(p^2q + pq^2) + 8(p^2 + q^2) + 28pq + 10(p + q) + 3$,

7. $S(G) = \frac{4}{3}\big[12(p^3q^2 + p^2q^3) + 28(p^3q + pq^3) + 84p^2q^2 + 16(p^3 + q^3) + 144(p^2q + pq^2) + 72(p^2 + q^2) + 205pq + 89(p + q) + 33\big]$,

8. $Gut(G) = \frac{2}{3}\big[32(p^3q^2 + p^2q^3) + 64(p^3q + pq^3) + 192p^2q^2 + 32(p^3 + q^3) + 283(p^2q + pq^2) + 120(p^2 + q^2) + 352pq + 130(p + q) + 42\big]$.

Proof. It is clear that $|V(G)| = 3pq + 4(p + q) + 5$ and $|E(G)| = 4(pq + p + q + 1)$. As already mentioned, every pendant edge (every bridge) forms a Θ^*-class. Moreover, removing the pendant edges from the SiO_2 layer structure of dimension (p, q), we obtain the graph that is the subdivision graph of the $(p + 1) \times (q + 1)$ square grid (alias the Cartesian product of P_{p+1} with P_{q+1}). As paths are partial cubes and Cartesian products of partial cubes are again partial cubes, Theorem 3 applies. Consequently, the Θ^*-classes of $E(G)$ formed in this structure are the horizontal, vertical and pendant edge cuts. We denote the pendant cuts as P_i, where $\{P_i : 1 \leq i \leq 2(p + q + 2)\}$ lie on the boundary of the structure, vertical cuts as V_i, where $\{V_i : 1 \leq i \leq q\}$ and horizontal cuts as H_i, where $\{H_i : 1 \leq i \leq p\}$. Therefore, there are $2(p + q + 2)$ pendant cuts, q vertical cuts and p horizontal cuts as shown in Fig. 3. The proof is now divided into three cases for computation. The quotient graph obtained after applying the cut has edge-strength value 1 in all the cases.

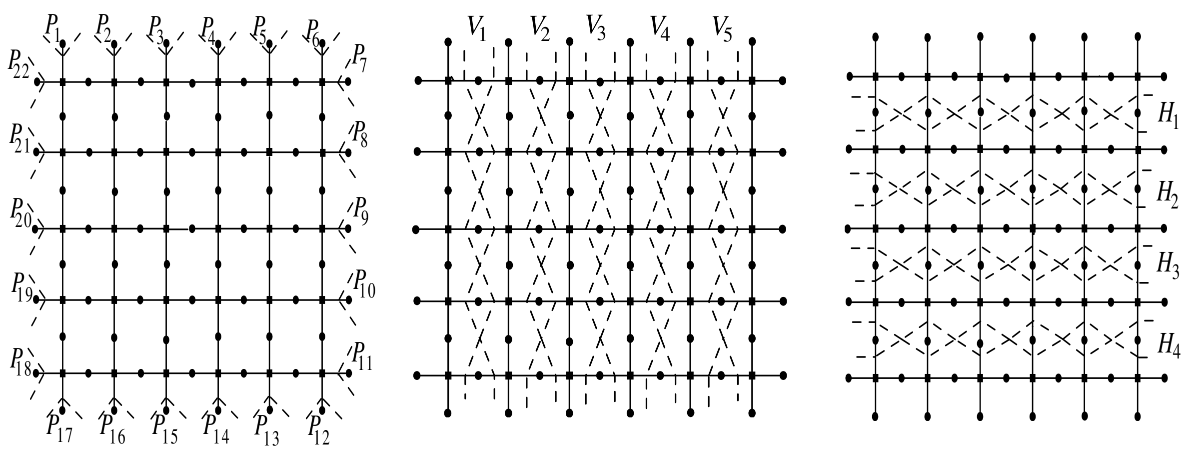

(a) (b) (c)

Figure 3: Convex cuts on G (a) P_i (b) V_i and (c) H_i

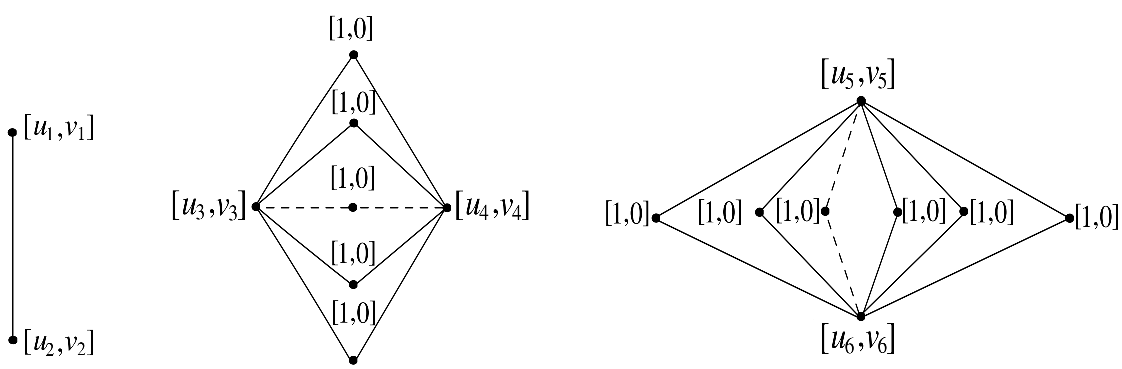

(a) (b) (c)

Figure 4: Quotient graphs (a) G/P_i, (b) G/V_i and (c) G/H_i

(i) $\boldsymbol{G/P_i}, \{\boldsymbol{P_i}, \mathbf{1} \leq \boldsymbol{i} \leq \boldsymbol{2(p+q+2)}\}$:

The edge-cut P_i of G and the quotient graph together with its corresponding strength-weighted function are shown in Figs. 3(a) and 4(a) respectively. Since all the $P_i's$ are symmetric to each other, it is enough to compute for a single cut. The quotient graph G/P_i obtained is a complete graph K_2 with vertex-strength-weighted values $[u_1, v_1]$ and $[u_2, v_2]$ where,

$u_1 = 1, \qquad v_1 = 0,$

$u_2 = |V(G)| - 1, \quad v_2 = |E(G)| - 1.$

Denote

$$TI(G_1) = TI(G/P_i, (w_v^i, s_v^i), s_e^i)\,. \tag{1}$$

(ii) $\boldsymbol{G/\,V_i}, \{\,\boldsymbol{V_i}, \mathbf{1} \leq \boldsymbol{i} \leq \boldsymbol{q}\}$:

Fig. 3(b) is the graph G with edge-cut V_i and Fig. 4(b) is the quotient graph G/V_i with its corresponding strength-weighted function. From Fig. 3(b), it is easy to see that cut V_1 is symmetric to cut V_q, cut V_2 is symmetric to cut V_{q-1}, cut V_3 is symmetric to cut V_{q-2} and so on. The quotient graph with cut $G/\,V_i$ is a bipartite graph $K_{2,p+1}$ as shown in Fig. 4(b) and the vertex-strength-weighted values are not defined given below:

$u_3 = (3p + 4)i, \qquad v_3 = (p + 1)(4i - 1),$

$u_4 = (3p + 4)(q + 1 - i), \quad v_4 = (p + 1)(4(q - i) + 3).$

Denote

$$TI(G_2) = TI(G/V_i, (w_v^i, s_v^i), s_e^i)\,. \tag{2}$$

(iii) $\boldsymbol{G/H_i}, \{\boldsymbol{H_i}, \mathbf{1} \leq \boldsymbol{i} \leq \boldsymbol{p}\}$:

The graph G with edge-cut H_i is shown in Fig. 3(c) and the quotient graph together with its corresponding strength-weighted function is shown in Fig. 4(c). Due to symmetry, this case becomes similar to the above case when p is replaced by q and vice-versa. The vertex-strength-weighted values of the quotient graph in this case are as follows:

$u_5 = (3q + 4)i, \qquad v_5 = (q + 1)(4i - 1),$

$u_6 = (3q + 4)(p + 1 - i), \quad v_6 = (q + 1)(4(p - i) + 3).$

Denote

$$TI(G_3) = TI(G/H_i, (w_v^i, s_v^i), s_e^i)\,. \tag{3}$$

From Eqs. (1)-(3) we have

$$TI(G) = 2(p+q+2)TI(G_1) + \sum_{i=1}^{q} TI(G_2) + \sum_{i=1}^{p} TI(G_3).$$

$$W(G) = u_1u_2 + (p+1)(u_3+u_4+pq) + 2u_3u_4 + (q+1)(u_5+u_6+pq) + 2u_5u_6.$$

$$SZ_v(G) = u_1u_2 + (p+1)(u_3+u_4+2u_3u_4+p(u_3+u_4)+2p) + (q+1)(u_5+u_6+2u_5u_6+ q(u_5+u_6)+2q).$$

$$SZ_e(G) = v_1v_2 + (p+1)(v_3+v_4+2v_3v_4+p(v_3+v_4)+2p) + (q+1)(v_5+v_6+2v_5v_6+ q(v_5+v_6)+2q).$$

$$SZ_{ev}(G) = u_1v_2 + u_2v_1 + \frac{(p+1)}{2}(u_3+u_4+v_3+v_4+p(u_3+u_4+v_3+v_4)+2(u_3v_4+u_4v_3) +4p) + \frac{(q+1)}{2}(u_5+u_6+v_5+v_6+q(u_5+u_6+v_5+v_6)+2(u_5v_6+u_6v_5)+4q).$$

$$SZ_t(G) = SZ_v(G) + SZ_e(G) + 2SZ_{ev}(G).$$

$$PI(G) = v_1+v_2+2(p+1)(v_3+v_4+p+1)+2(q+1)(v_5+v_6+q+1).$$

$$S(G) = 2(u_1v_2+u_2v_1+u_1+u_2) + 2(p+1)(u_3+u_4+v_3+v_4+2pq+p+1) + 2(2(u_3v_4+ u_4v_3)+u_3p+u_4p+u_3+u_4) + 2(q+1)(u_5+u_6+v_5+v_6+2pq+q+1) + 2(2(u_5v_6 +u_6v_5)+u_5q+u_6q+u_5+u_6).$$

$$Gut(G) = 4v_1v_2+2v_1+2v_2+1+2(p+1)(2v_3+p+1)(2v_4+p+1)+2(4v_3v_4+2p(v_3+v_4) +2(v_3+v_4)+(p+1)^2+2pq(p+1))+2(q+1)(2v_5+q+1)(2v_6+q+1)+2(4v_5v_4 +2q(v_5+v_6)+2(v_5+v_6)+(q+1)^2+2pq(q+1)).$$

The results are obtained on substituting the values of the parameters. □

The analytical closed formulae presented in Theorem 4 are polynomials in two variables, where $PI(G)$ is a degree-4 polynomial, $W(G)$, $S(G)$, and $Gut(G)$ are degree-5 polynomial, while the four expressions for the Szeged indices are degree-6 polynomials. Hence asymptotically the Szeged indices dominate the other indices, and each of the Wiener, the Schultz and the Gutman index dominates the PI index. If two polynomials are of the same degree, then their asymptotic behaviors are determined by the corresponding leading coefficient. For instance,

$$\lim_{p,q\to\infty} \frac{W(G)}{S(G)} = \frac{18/3}{96/3} = \frac{3}{16}\,,$$

and

$$\lim_{p,q\to\infty} \frac{SZ_v(G)}{Sz_e(G)} = \frac{18/3}{32/3} = \frac{9}{16}\,.$$

The other limit quotients can be deduced analogously.

In all our next theorems the above assertions about the degree of the derived polynomials will be parallel to the ones from Theorem 4. Hence we will not repeat the above conclusions.

4.2 Topological indices of C_8 layer structure

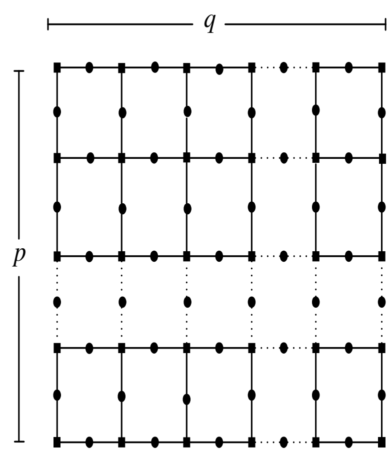

Figure 5: C_8 layer structure

We now form a new structure named as the C_8 layer structure of dimension (p, q) by deleting the pendant vertices and its corresponding edges from the SiO_2 layer structure of dimension (p, q) to form an octagonal mesh as shown in Fig. 5. In this structure, we have $|V(G)| = 3pq + 2(p + q) + 1$ and $|E(G)| = 4pq + 2(p + q)$. The distance-based topological indices of the C_8 layer structure are computed as follows.

Theorem 5. *Let G be a* C_8 *layer structure of dimension* (p,q)*,* $p,q \geq 1$*.*

1. $W(G) = \frac{1}{3}\big[9(p^3q^2 + p^2q^3) + 12(p^3q + pq^3) + 36p^2q^2 + 4(p^3 + q^3) + 33(p^2q + pq^2) + 6(p^2 + q^2) + 24pq + 2(p+q)\big]$,

2. $SZ_v(G) = \frac{1}{3}\big[18p^3q^3 + 39(p^3q^2 + p^2q^3) + 25(p^3q + pq^3) + 78p^2q^2 + 4(p^3 + q^3) + 51(p^2q + pq^2) + 6(p^2 + q^2) + 34pq + 2(p+q)\big]$,

3. $SZ_e(G) = \frac{2}{3}\big[16p^3q^3 + 22(p^3q^2 + p^2q^3) + 14(p^3q + pq^3) + 6p^2q^2 + 2(p^3 + q^3) + 2(p^2q + pq^2) - 3(p^2 + q^2) + 10pq + (p+q)\big]$,

4. $SZ_{ev}(G) = \frac{1}{6}\big[48p^3q^3 + 85(p^3q^2 + p^2q^3) + 51(p^3q + pq^3) + 108p^2q^2 + 8(p^3 + q^3) + 53(p^2q + pq^2) + 30pq - 2(p+q)\big]$,

5. $SZ_t(G) = \frac{2}{3}\big[49p^3q^3 + 84(p^3q^2 + p^2q^3) + 52(p^3q + pq^3) + 99p^2q^2 + 8(p^3 + q^3) + 54(p^2q + pq^2) + 42pq + (p+q)\big]$,

6. $PI(G) = 2\big[4p^2q^2 + 4pq^3 + q^3 + p^2q + 12pq^2 + 2q^2 + 2pq - 2q\big]$,

7. $S(G) = \frac{2}{3}\big[24(p^3q^2 + p^2q^3) + 28(p^3q + pq^3) + 84p^2q^2 + 8(p^3 + q^3) + 63(p^2q + pq^2) + 6(p^2 + q^2) + 40pq + (p+q)\big]$,

8. $Gut(G) = \frac{2}{3}\big[32(p^3q^2+p^2q^3)+32(p^3q+pq^3)+96p^2q^2+8(p^3+q^3)+55(p^2q+pq^2)+32pq+(p+q)\big]$.

Proof. Proceeding as in the proof of Theorem 4 (again applying Theorem 3), we obtain vertical and horizontal Θ^*-classes of $E(G)$. The vertical and horizontal cuts are denoted as V_i, where $\{V_i : 1 \leq i \leq q\}$ and H_i, where $\{H_i : 1 \leq i \leq p\}$ respectively.

The graph G with edge-cut V_i and the quotient graph with corresponding strength-weighted functions are depicted in Figs. 6(a) and 4(b). The vertex-strength-weighted values $[u_3, v_3]$ and $[u_4, v_4]$ are replaced as follows:

$u_3 = p(3i-1) + (2i-1)$, $\quad v_3 = 2i(2p+1) - 2(p+1)$,

$u_4 = 3p(q-i) + 2(p+q-i) + 1$, $\quad v_4 = (4p+2)(q-i) + 2p$.

Now,

$$TI(G_4) = TI(G/V_i, (w_v^i, s_v^i), s_e^i)\,. \tag{4}$$

In a similar way, the graph G with edge-cut H_i and the quotient graph together with its corresponding strength-weighted function are shown in Figs. 6(b) and 4(c) respectively. The vertex-strength-weighted values $[u_5, v_5]$ and $[u_6, v_6]$ are replaced as

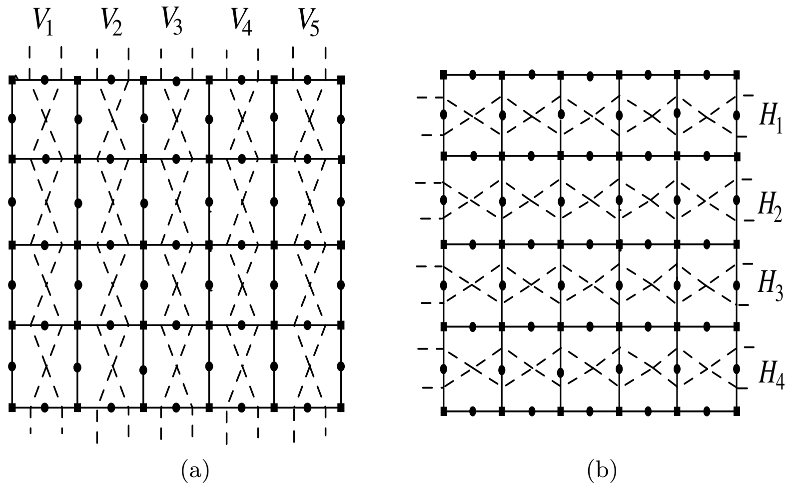

Figure 6: Convex cuts on C_8 layer structure (a) V_i (b) H_i

$$u_5 = q(3i-1) + (2i-1), \qquad v_5 = 2i(2q+1) - 2(q+1),$$
$$u_6 = 3q(p-i) + 2(p+q-i) + 1, \quad v_6 = (4q+2)(p-i) + 2q,$$

and now we have

$$TI(G_5) = TI(G/H_i, (w_v^i, s_v^i), s_e^i)\,. \tag{5}$$

The edge-strength values in $TI(G_4)$ and $TI(G_5)$ are 1 each. Therefore, from Eqs. (4)-(5),

$$TI(G) = \sum_{i=1}^{q} TI(G_4) + \sum_{i=1}^{p} TI(G_5)\,.$$

Following the approach from the proof of Theorem 4 we obtain the desired result. □

4.3 Topological indices of SiO_2 nanotube

Silica nanotubes exhibit empty inner space which can be filled by functional loads. In addition, the mesoporous silica surface is hydrophilic, lends to functionalization and biocompatible so that the material can be applied in bioseparation, biocatalysis, biosensoring, drug/gene delivery carriers, adsorption, select sequestration, drug delivery and controlled release [21, 45, 52]. In this section, we compute the topological indices of SiO_2 nanotube structure that we construct from the known structures of SiO_2 sheets. Consequently, in graph-theoretical terms, we form an SiO_2 nanotube of dimension (p, q) by merging all the pendant vertices along right and left sides of SiO_2 layer structure of dimension $(p, q-1)$ forming a tubular structure of the nanotube with length p and circumference q as shown in Fig. 7. From the structure, we have $|V(G)| = q(3p+4)$ and $|E(G)| = 4q(p+1)$.

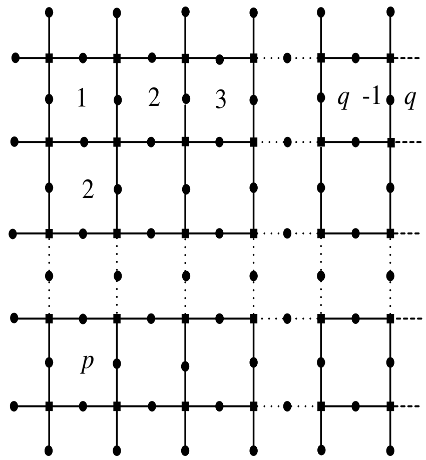

Figure 7: SiO_2 nanotube (p, q)

Theorem 6. *Let G be an SiO_2 nanotube of dimension (p, q), where $p \geq 1, q \geq 2$ and q is odd.*

1. $W(G) = \frac{1}{4}\big[3(4p^3q^2 + 3p^2q^3) + 48p^2q^2 + 24pq^3 + 16q^3 + 3p^2q + 64pq^2 + 32q^2 - 4pq - 12q\big]$,

2. $SZ_v(G) = \frac{1}{2}\big[15p^3q^3 + 57p^2q^3 - 9p^3q + 58pq^3 + 16q^3 - 21p^2q + 16pq^2 + 16q^2 - 20pq - 8q\big]$,

3. $SZ_e(G) = \frac{2}{3}\big[20p^3q^3 - 3(4p^3q^2 - 18p^2q^3) - 9p^3q + 46pq^3 - 36p^2q^2 + 12q^3 - 3(5p^2q + 11pq^2) - 9pq - 12q^2\big]$,

4. $SZ_{ev}(G) = \frac{1}{2}\big[20p^3q^3 - 6p^3q^2 + 65p^2q^3 - 12p^3q + 59pq^3 - 20p^2q^2 + 16q^3 - 2(13p^2q + 5pq^2) - 22pq - 6q\big]$,

5. $SZ_t(G) = \frac{1}{6}\big[245p^3q^3 - 3(28p^3q^2 + 259p^2q^3) - 135p^3q + 712pq^3 - 264p^2q^2 + 192q^3 - 9(31p^2q + 16pq^2) - 228pq - 60q\big]$,

6. $PI(G) = 2\big[8p^2q^2 - 2p^2q + 15pq^2 + 8q^2 - 4pq - 3q\big]$,

7. $S(G) = 2\big[2(4p^3q^2 + 3p^2q^3) + 14pq^3 + 28p^2q^2 + 8q^3 + p^2q + 32pq^2 + 12q^2 - 3pq - 4q\big]$,

8. $Gut(G) = \frac{2}{3}\big[8(4p^3q^2 + 3p^2q^3) + 48pq^3 + 96p^2q^2 + 24q^3 + 91pq^2 - 12pq + 24q^2 - 9q\big]$.

Proof. Again, each pendant edge forms its own Θ^*-class. Let these pendant edge-cuts be denoted as P_i, $\{P_i : 1 \leq i \leq 2q\}$, see Fig. 8(a). Removing these pendant edges, we obtain the subdivision graph of the Cartesian product of a path with an odd cycle. Since this graph is not a partial cube (in particular, it is not bipartite), we cannot apply Theorem 3. However, by a direct checking we can verify that we obtain vertical and horizontal Θ^*-classes as follows. Since q is odd, there is a unique

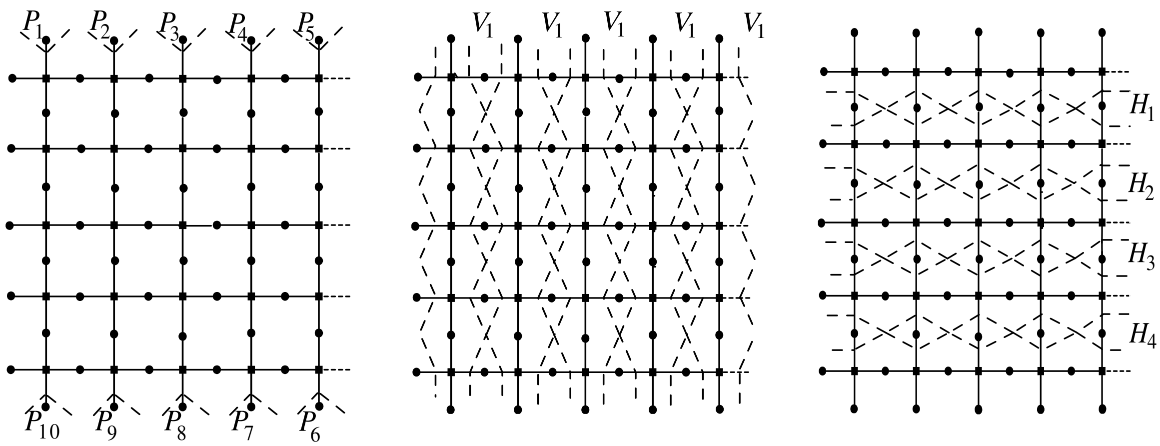

(a) (b) (c)

Figure 8: Convex cuts on G (a) P_i (b) V_1 and (c) H_i

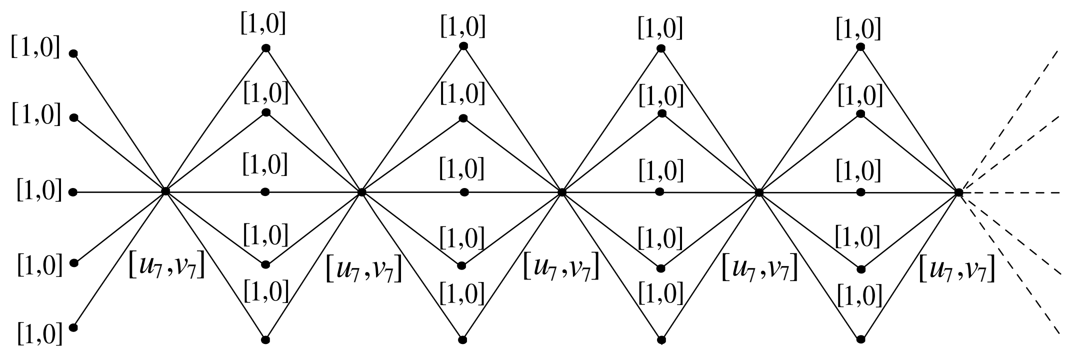

Figure 9: Quotient graph G/V_1

vertical Θ^*-class which is denoted as V_1, see Fig. 8(b). Horizontal cuts are H_i, $\{H_i : 1 \leq i \leq p\}$, see Fig. 8(c). The quotient graph thus obtained has an edge-strength value of 1.

(i) $\boldsymbol{G/P_i, \{P_i, 1 \leq i \leq 2q\}}$:

The graph G with edge cut P_i and the quotient graph together with its corresponding strength-weighted functions are shown in Figs. 8(a) and 4(a), respectively. It is enough to compute for a single cut due to symmetry of all the P_i's. The quotient graph G/P_i obtained is a complete graph K_2 with vertex-strength-weighted values $[u_1, v_1], [u_2, v_2]$ where

$u_1 = 1, \qquad v_1 = 0,$

$u_2 = |V(G)| - 1, \quad v_2 = |E(G)| - 1.$

Denote

$$TI(G_6) = TI(G/P_i, (w_v^i, s_v^i), s_e^i)\,. \tag{6}$$

(ii) $\boldsymbol{G/V_1}$:

The graph G with edge-cut V_1 and its quotient graph are shown in Figs. 8(b) and 9 respectively. The quotient graph has vertex-strength-weighted values as follows:

$u_7 = 2p + 3, \quad v_7 = 2p + 2,$

Now,

$$TI(G_7) = TI(G/V_1, (w_v^1, s_v^1), s_e^1)\,. \tag{7}$$

(iii) $\boldsymbol{G/H_i, \{H_i, 1 \le i \le p\}}$:

The graph G with edge-cut H_i and the quotient graph are shown in Figs. 8(c) and 4(c) respectively. The quotient graph is a bipartite graph $K_{2,q+1}$ with vertex-strength-weighted values replaced as follows: $\begin{array}{ll} u_5 = 3qi, & v_5 = q(4i-1), \\ u_6 = 3q(p+1-i), & v_6 = q(4p-4i+3). \end{array}$ Now,

$$TI(G_8) = TI(G/H_i, (w_v^i, s_v^i), s_e^i)\,. \tag{8}$$

From Eqs. (6)-(8) we get

$$TI(G) = 2qTI(G_6) + TI(G_7) + \sum_{i=1}^{p} TI(G_8)\,.$$

We obtain the desired result by substituting the values of the parameters. □

Theorem 7. *Let G be an SiO_2 nanotube of dimension (p, q), where $p \ge 1, q \ge 2$ and q is even.*

1. $W(G) = \frac{1}{4}\big[3(4p^3q^2 + 3p^2q^3) + 24pq^3 + 48p^2q^2 + 16q^3 + 4(p^2q + 16pq^2) + 32q^2 - 8q\big]$,
2. $SZ_v(G) = \frac{1}{2}\big[15p^3q^3 + 57p^2q^3 - 4p^3q + 58pq^3 + 16pq^2 + 16q^3 - 4p^2q + 16q^2 - 4pq - 4q\big]$,
3. $SZ_e(G) = \frac{2}{3}\big[20p^3q^3 - 6(2p^3q^2 - 9p^2q^3) + 46pq^3 - 36p^2q^2 + 12q^3 + 3(2p^2q - 11pq^2) - 12q^2 + 6pq + 3q\big]$,
4. $SZ_{ev}(G) = \frac{1}{2}\big[20p^3q^3 - 6p^3q^2 + 65p^2q^3 - 4p^3q + 59pq^3 - 20p^2q^2 + 16q^3 - 2(2p^2q + 5pq^2) - 4pq - 2q\big]$,
5. $SZ_t(G) = \frac{1}{6}\big[245p^3q^3 - 3(28p^3q^2 - 259p^2q^3) - 4(9p^3q - 178pq^3) - 264p^2q^2 + 192q^3 - 12(p^2q + 12pq^2) - 12pq - 12q\big]$,

6. $PI(G) = 2\left[8p^2q^2 - 2p^2q + 15pq^2 + 8q^2 - 4pq - 3q\right]$,

7. $S(G) = 4\left[4p^3q^2 + 3p^2q^3 + 7pq^3 + 14p^2q^2 + 4q^3 + p^2q + 16pq^2 + 6q^2 - q\right]$,

8. $Gut(G) = \frac{2}{3}\left[4(8p^3q^2 + 6p^2q^3) + 48pq^3 + 96p^2q^2 + 24q^3 + 6p^2q + 91pq^2 + 24q^2 - 3q\right]$.

Proof. We know that $|V(G)| = q(3p+4)$ and $|E(G)| = 4q(p+1)$. After removing the pendant edges that form their own Θ^*-classes, we are left with the Cartesian product of a path with an even cycle. This is always a partial cube, hence Theorem 3 applies again. The vertical cuts are denoted as V_i, $\{V_i : 1 \leq i \leq \frac{q}{2}\}$, while the pendant and horizontal edge-cuts follow the same lines as in the proof of Theorem 6.

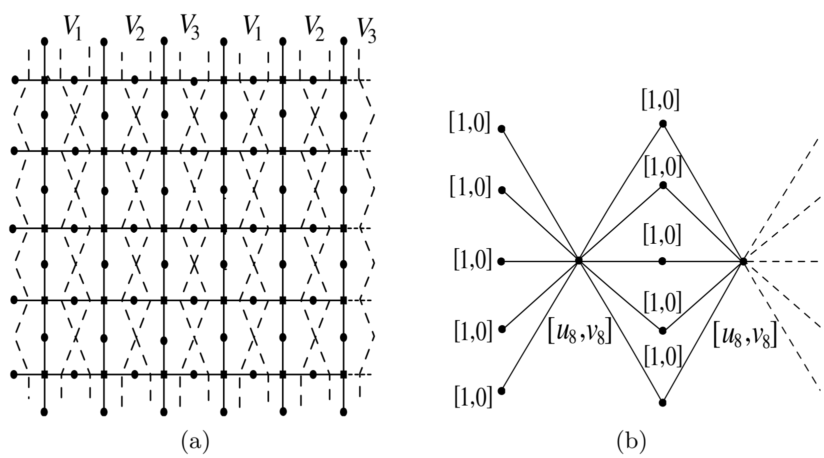

Figure 10: (a) Convex cut V_i and (b) Quotient graph G/V_i

Figs. 10(a) and 10(b) depict the graph G with edge cut V_i and the quotient graph together with its corresponding strength-weighted function respectively. The edge-strength value is 1 and the vertex-strength-weighted values are as follows: $u_8 = \frac{3pq}{2} + 2q - (p+1)$, $v_8 = 2(pq + q - p - 1)$, Now,

$$TI(G_9) = TI(G/V_i, (w_v^i, s_v^i), s_e^i)\,. \tag{9}$$

Therefore,

$$TI(G) = 2qTI(G_6) + \frac{q}{2}TI(G_9) + \sum_{i=1}^{p} TI(G_8)\,.$$

By substituting the values of the parameters we obtain the desired result. □

Table 3: Asymptotic behaviors of SiO_2 nanotube

TI	**SiO_2 nanotube**		
	$p \to \infty$		$q \to \infty$
	q odd	q even	q odd or even
W	$3p^3q^2$		$q^3(9p^2 + 24p + 16)/4$
SZ_v	$p^3(15q^3 - 9q)/2$	$p^3(15q^3 - 4q)/2$	$q^3(15p^3 + 57p^2 + 58p + 16)/2$
SZ_e	$p^3(40q^3 - 24q^2 - 18q)/3$	$p^3(40q^3 - 24q^2)/3$	$q^3(40p^3 + 108p^2 + 92p + 24)/3$
SZ_{ev}	$p^3(10q^3 - 3q^2 - 6q)$	$p^3(10q^3 - 3q^2 - 2q)$	$q^3(20p^3 + 65p^2 + 59p + 16)/2$
SZ_t	$p^3(245q^3 - 84q^2 - 135q)/6$	$p^3(245q^3 - 84q^2 - 36q)/6$	$q^3(245p^3 + 777p^2 + 712p + 192)/6$
PI	$p^2(16q^2 - 4q)$		$q^2(16p^2 + 30p + 16)$
S	$16p^3q^2$		$q^3(12p^2 + 28p + 16)$
Gut	$64p^3q^2/3$		$q^3(16p^2 + 32p + 16)$

When the length p and circumference q are tending to large values, all the variants of Szeged and PI indices become asymptotic to p^3q^3 and p^2q^2 as leading terms respectively, while the other indices increase indefinitely as shown in Table 3.

4.4 Topological indices of SiO_2 nanotori

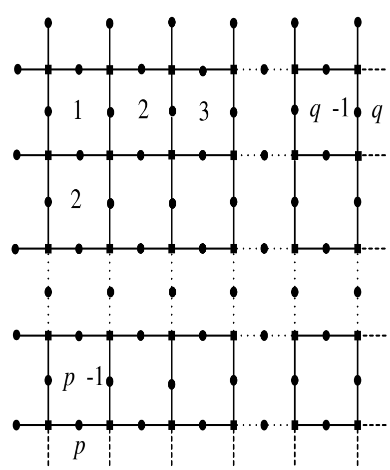

Figure 11: SiO_2 nanotori (p, q)

Although the exact chemical structures of SiO_2 nanotori are unknown at present time, SiO_2 nanotori have been patented [51] and colloidal plasmonic gold nanotori and nanorings have been observed in pulsed laser photophysical applications [1, 34]. A primary motivation for such studies is that such nanorings and nanotori find novel applications in efficient photothermal drug delivery. When SiO_2 nanotube of dimension $(p-1, q)$ is bent into a ring, it forms a doughnut shaped structure and we name it as SiO_2 nanotori of dimension (p, q) which is shown in Fig. 11. Clearly, we have $|V(G)| = 3pq$ and $|E(G)| = 4pq$. We further proceed to compute the topological indices of SiO_2 nanotori.

Theorem 8. *For $p, q \geq 2$, let G be an SiO_2 nanotori of dimension (p, q), where p and q are odd.*

1. $W(G) = \frac{1}{4}\left[9(p^3q^2 + p^2q^3) + 3(p^2q + pq^2) - 8pq\right]$,
2. $SZ_v(G) = \frac{1}{2}\left[18p^3q^3 - 9(p^3q + pq^3) + 12(p^2q + pq^2) - 8pq\right]$,
3. $SZ_e(G) = 2\left[8p^3q^3 - 4(p^3q^2 + 4p^2q^3) - 3(p^3q + pq^3) + 4(p^2q + pq^2) - 2pq\right]$,
4. $SZ_{ev}(G) = 12p^3q^3 - 3(p^3q^2 + p^2q^3) - 6(p^3q + pq^3) + 7(p^2q + pq^2) - 4pq$,
5. $SZ_t(G) = \frac{1}{2}\left[98p^3q^3 - 28(p^3q^2 + p^2q^3) - 45(p^3q + pq^3) + 56(p^2q + pq^2) - 32pq\right]$,
6. $PI(G) = 4\left[4p^2q^2 - (p^2q + pq^2)\right]$,
7. $S(G) = 2\left[6(p^3q^2 + p^2q^3) + (p^2q + pq^2) - 4pq\right]$
8. $Gut(G) = 8\left[2(p^3q^2 + p^2q^3) - pq\right]$.

Proof. By applying Θ^* relation, we obtain horizontal and vertical edge-cuts of $E(G)$. Since p and q are odd, the number of horizontal and vertical cuts are just 1 each and are denoted as H_1 and V_1 respectively. The quotient graph for both the cuts have the edge-strength values of 1.

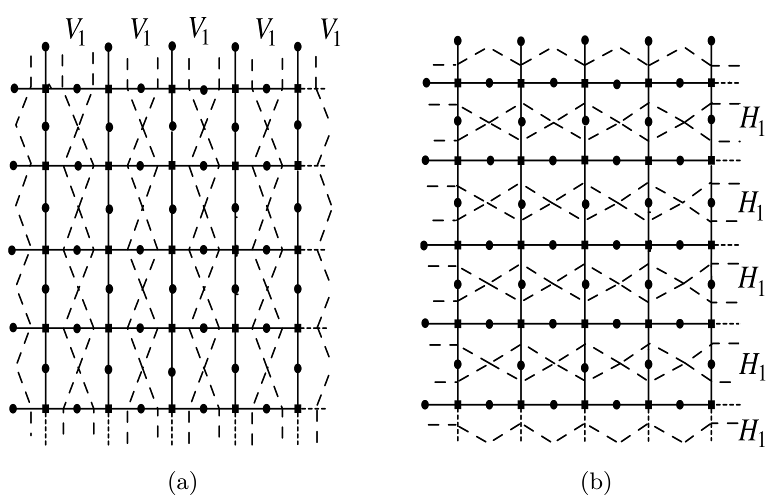

Figure 12: Convex cuts on G (a) V_1 and (b) H_1

(i) $\boldsymbol{G/V_1}$:

Figs. 12(a) and 9 represent the graph G with edge cut V_1 and the quotient graph together with its corresponding strength-weighted function respectively. The quotient graph G/V_1 has vertex-strength-weighted values $[u_7, v_7]$ where, $u_7 = 2p, \quad v_7 = 2p,$ Denote

$$TI(G_{10}) = TI(G/V_1, (w_v^1, s_v^1), s_e^1)\,. \tag{10}$$

(ii) $\boldsymbol{G/H_1}$:

Figs. 12(b) and 9 represent the graph G with edge cut H_1 and the quotient graph together with its corresponding strength-weighted function respectively. This case is similar to the above case with vertex-strength-weighted values $[u_7, v_7]$ replaced as $u_7 = 2q, \quad v_7 = 2q,$ Now,

$$TI(G_{11}) = TI(G/H_1, (w_v^1, s_v^1), s_e^1)\,. \tag{11}$$

From Eqs. (10) and (11) we get

$$TI(G) = TI(G_{10}) + TI(G_{11})\,.$$

By substituting the values of the parameters in the above equation we obtain the desired result. □

Theorem 9. *For $p, q \geq 2$, let G be an* SiO_2 *nanotori of dimension (p, q), where p and q are even.*

1. $W(G) = \frac{1}{4}\big[9(p^3q^2 + p^2q^3) + 4(p^2q + pq^2) - 8pq\big]$,
2. $SZ_v(G) = 9p^3q^3 - 2(p^3q + pq^3) + 4(p^2q + pq^2) - 4pq$,
3. $SZ_e(G) = 16p^3q^3 - 8(p^3q^2 + p^2q^3) + 4(p^2q + pq^2) - 4pq$,
4. $SZ_{ev}(G) = 12p^3q^3 - 3(p^3q^2 + p^2q^3) - 2(p^3q + pq^3) + 4(p^2q + pq^2) - 4pq$,
5. $SZ_t(G) = 49p^3q^3 - 14(p^3q^2 + p^2q^3) - 6(p^3q + pq^3) + 16(p^2q + pq^2) - 16pq$,
6. $PI(G) = 4\big[4p^2q^2 - (p^2q + pq^2)\big]$,
7. $S(G) = 4\big[3(p^3q^2 + p^2q^3) + (p^2q + pq^2) - 2pq\big]$,
8. $Gut(G) = 4\big[4(p^3q^2 + p^2q^3) + (p^2q + pq^2) - 2pq\big]$.

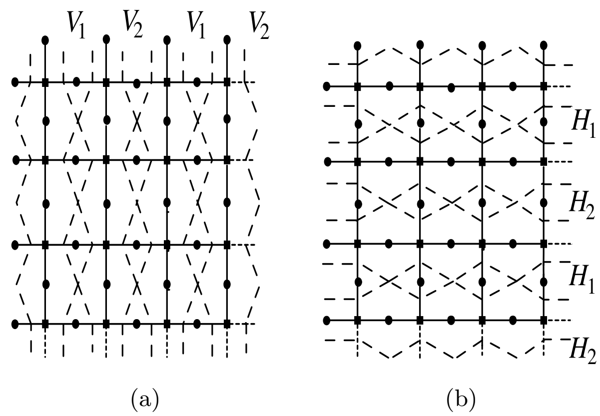

Figure 13: Convex cuts on G (a) V_i and (b) H_i

Proof. The Θ^*-classes of $E(G)$ obtained here are horizontal and vertical edge-cuts. Since p and q are even, Theorem 3 applies because we have the subdivision graph of the Cartesian product of two even cycles. The number of vertical cuts which are denoted as V_i is $\frac{q}{2}$, and the number of horizontal cuts, denoted as H_i, is $\frac{p}{2}$. The quotient graph obtained takes edge-strength value 1.

(i) $G/V_i, 1 \leq i \leq q/2$:

Figs. 13(a) and 10(b) represent the graph G with edge cut V_i and its corresponding quotient graph respectively. The vertex-strength-weighted values $[u_8, v_8]$ in the quotient graph G/V_i are $u_8 = \frac{3}{2}pq - p, \quad v_8 = 2pq - 2p,$ Denote

$$TI(G_{12}) = TI(G/V_i, (w_v^i, s_v^i), s_e^i) \,. \tag{12}$$

(ii) $G/H_i, 1 \leq i \leq p/2$:

Figs. 13(b) and 10(b) represent the graph G with edge cut H_i and its corresponding quotient graph respectively. The vertex-strength-weighted values $[u_8, v_8]$ are replaced as $u_8 = \frac{3}{2}pq - q, \quad v_8 = 2pq - 2q,$ Denote

$$TI(G_{13}) = TI(G/H_i, (w_v^i, s_v^i), s_e^i) \,. \tag{13}$$

From Eqs. (12) and (13) we get

$$TI(G) = \frac{q}{2}TI(G_{12}) + \frac{p}{2}TI(G_{13}) \,.$$

We obtain the desired result by substituting the values of the parameter. □

Theorem 10. *For $p, q \geq 2$, let G be an SiO_2 nanotori of dimension (p, q), where p is even and q is odd.*

1. $W(G) = \frac{1}{4}\big[9(p^3q^2 + p^2q^3) + 3p^2q + 4pq^2 - 8pq\big]$,
2. $SZ_v(G) = \frac{1}{2}\big[18p^3q^3 - 9p^3q - 4pq^3 + 4(3p^2q + 2pq^2) - 8pq\big]$,
3. $SZ_e(G) = 2\big[8p^3q^3 - 4(p^3q^2 + p^2q^3) - 3p^3q + 2(2p^2q + pq^2) - 2pq\big]$,
4. $SZ_{ev}(G) = 12p^3q^3 - 3(p^3q^2 + p^2q^3) - 2(3p^3q + pq^3) + 7p^2q + 4pq^2 - 4pq$,
5. $SZ_t(G) = \frac{1}{2}\big[(98p^3q^3 - 28(p^3q^2 + p^2q^3) - 3(15p^3q + 4pq^3) + 8(7p^2q + 4pq^2) - 32pq\big]$,
6. $PI(G) = 4\big[4p^2q^2 - (p^2q + pq^2)\big]$,
7. $S(G) = 2\big[6(p^3q^2 + p^2q^3) + p^2q + 2pq^2 - 4pq\big]$,
8. $Gut(G) = 4\big[4(p^3q^2 + p^2q^3) + pq^2 - 2pq\big]$.

Proof. The vertical and horizontal edge-cuts obtained upon applying Θ^* relation follow the same proof lines as in Case (i) of Theorem 8 and Case (ii) of Theorem 9 respectively. Therefore,

$$TI(G) = TI(G_{10}) + \frac{p}{2}TI(G_{13}),$$

and proceeding along the parallel lines as before we obtain the result. □

Theorem 11. *For $p, q \geq 2$, let G be an SiO_2 nanotori of dimension (p, q), where p is odd and q is even.*

1. $W(G) = \frac{1}{4}\big[9(p^3q^2 + p^2q^3) + 4p^2q + 3pq^2 - 8pq\big]$,
2. $SZ_v(G) = \frac{1}{2}\big[18p^3q^3 - 4p^3q - 9pq^3 + 4(2p^2q + 3pq^2) - 8pq\big]$,
3. $SZ_e(G) = 2\big[8p^3q^3 - 4(p^3q^2 + p^2q^3) - 3pq^3 + 2(p^2q + 2pq^2) - 2pq\big]$,
4. $SZ_{ev}(G) = 12p^3q^3 - 3(p^3q^2 + p^2q^3) - 2(p^3q + 3pq^3) + 4p^2q + 7pq^2 - 4pq$,
5. $SZ_t(G) = \frac{1}{2}\big[98p^3q^3 - 28(p^3q^2 + p^2q^3) - 3(4p^3q + 15pq^3) + 8(4p^2q + 7pq^2) - 32pq\big]$,
6. $PI(G) = 4\big[4p^2q^2 - (p^2q + pq^2)\big]$,
7. $S(G) = 2\big[6(p^3q^2 + p^2q^3) + 2p^2q + pq^2 - 4pq\big]$,

8. $Gut(G) = 4\left[4(p^3q^2 + p^2q^3) + p^2q - 2pq\right]$.

Proof. Following the same proof lines of Case (i) of Theorem 9 and Case (ii) of Theorem 8, we obtain the vertical and horizontal edge-cuts respectively. Then,

$$TI(G) = TI(G_{11}) + \frac{q}{2}TI(G_{12})$$

and the formulae follow as earlier. □

Table 4: Asymptotic behaviors of SiO_2 nanotori

TI	**SiO_2 nanotori**			
	$p \to \infty$		$q \to \infty$	
	q odd	q even	p odd	p even
W	$9p^3q^2/4$		$9p^2q^3/4$	
SZ_v	$p^3(18q^3 - 9q)/2$	$p^3(9q^3 - 2q)$	$q^3(18p^3 - 9p)/2$	$q^3(9p^3 - 2p)$
SZ_e	$p^3(16q^3 - 8q^2 - 6q)$	$p^3(16q^3 - 8q^2)$	$q^3(16p^3 - 8p^2 - 6p)$	$q^3(16p^3 - 8p^2)$
SZ_{ev}	$p^3(12q^3 - 3q^2 - 6q)$	$p^3(12q^3 - 3q^2 - 2q)$	$q^3(12p^3 - 3p^2 - 6p)$	$q^3(12p^3 - 3p^2 - 2p)$
SZ_t	$p^3(98q^3 - 28q^2 - 45q)/2$	$p^3(49q^3 - 14q^2 - 6q)$	$q^3(98p^3 - 28p^2 - 45p)/2$	$q^3(49p^3 - 14p^2 - 6p)$
PI	$p^2(16q^2 - 4q)$		$q^2(16p^2 - 4p)$	
S	$12p^3q^2$		$12p^2q^3$	
Gut	$16p^3q^2$		$16p^2q^3$	

As already mentioned earlier, and as can also be seen from Table 4, the leading term of the polynomials for the variants of the Szeged and for the PI index are p^3q^3 and p^2q^2, respectively, while the other three indices grow like degree-5 polynomials. A comparative analysis of various topological indices of SiO_2 nanostructures is shown in Fig. 14.

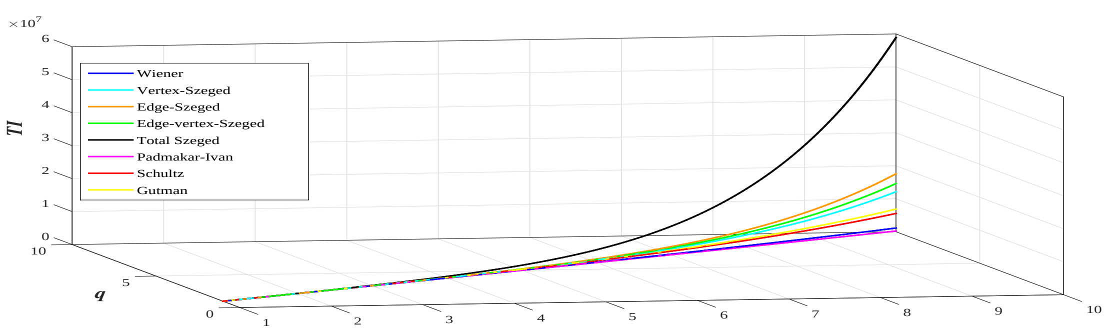

(a)

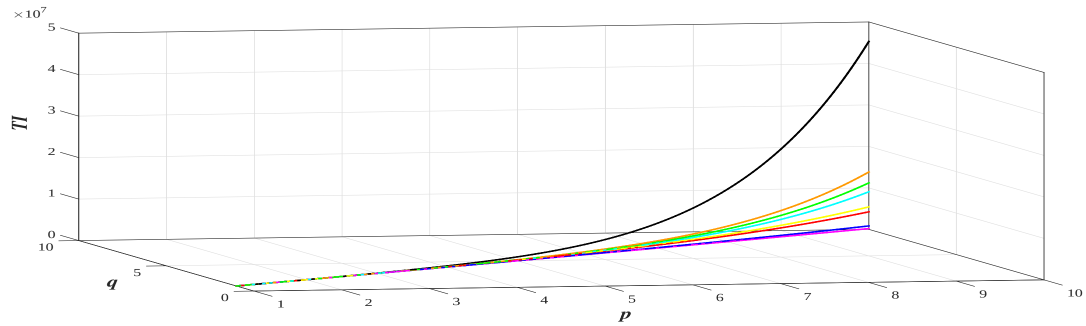

(b)

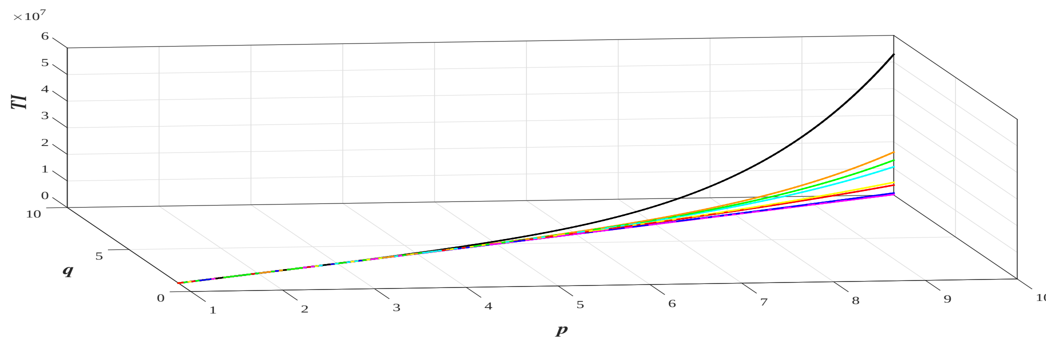

(c)

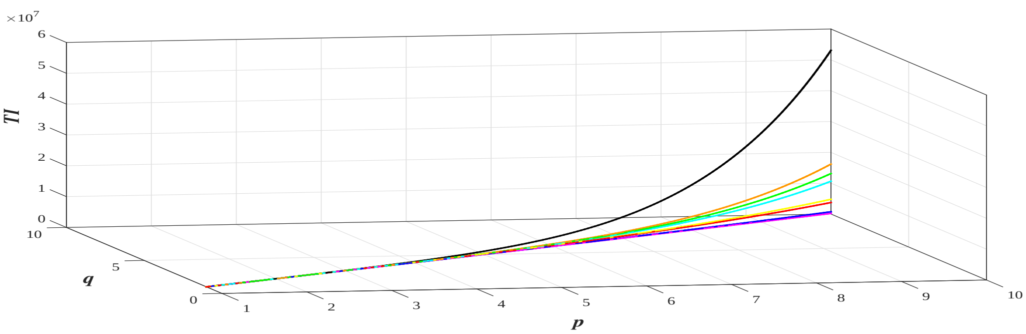

(d)

Figure 14: Comparative analysis of the topological indices (a) SiO_2 nanosheet (b) C_8 nanosheet (c) SiO_2 nanotube (d) SiO_2 nanotori

5 Conclusion

In this paper, we have obtained exact analytical expressions of various distance-based topological indices for SiO_2 nanosheets, nanotubes and nanotori. We have applied the cut method and reduced the original structure to strength-weighted quotient graphs and then computed the topological indices for these quotient graphs are also found to satisfy the original structure. SiO_2 nanostructures have various applications in the emerging field of nanobiomedicine for efficient drug delivery because of the optimal pore sizes and rediness for surface functionalization that such nano and mesoporous silicates posses. The results obtained in this paper could play a vital role in the design of QSAR/QSPR relationships for SiO_2 nanostructure.

References

[1] F. Alali, I.H. Karampelas, Y.H. Kim, E.P. Furlani, Photonic and thermofluidic analysis of colloidal plasmonic nanorings and nanotori for pulsed-laser photothermal applications, J. Phys. Chem. C **117**(39) (2013) 20178–20185.

[2] M. Arockiaraj, J. Clement, K. Balasubramanian, Topological indices and their applications to circumcised donut benzenoid systems, kekulenes and drugs, Polycycl. Aromat. Comp. DOI: 10.1080/10406638.2017.1411958.

[3] A.T. Balaban, Applications of graph theory in chemistry, J. Chem. inf. Comput. Sci. **25**(3) (1985) 334–343.

[4] A.T. Balaban, I. Motoc, D. Bonchev, O. Mekenyan, Topological indices for structure-activity correlations, Top. Curr. Chem. **114** (1983) 21–55.

[5] K. Balasubramanian, A method for nuclear spin statistics in molecular spectroscopy, J. Chem. Phys. **74**(12) (1981) 6824–6829.

[6] K. Balasubramanian, Spectra of chemical trees, Int. J. Quantum Chem. **21**(3) (1982) 581–590.

[7] K. Balasubramanian, Operator and algebraic methods for NMR spectroscopy. I. Generation of NMR spin species, J. Chem. Phys. **78**(11) (1983) 6358–6368.

[8] K. Balasubramanian, Applications of combinatorics and graph theory to spectrosocpy and quantum chemistry, Chem. Rev. **85**(6) (1985) 599–618.

[9] K. Balasubramanian, Characteristic polynomials of organic polymers and periodic structure, J. Comput. Chem. **6**(6) (1985) 656–661.

[10] K. Balasubramanian, Tree pruning and lattice statistics on Bethe lattices, J. Math. Chem. **2**(1) (1988) 69–82.

[11] K. Balasubramanian, Nuclear-spin statistics of C_{60}, $C_{60}H_{60}$ and $C_{60}D_{60}$, Chem. Phys. lett. **183**(3-4) (1991) 292–296.

[12] K. Balasubramanian, Exhaustive generation and analytical expressions of matching polynomials of fullerenes C_{20}-C_{50}, J. Chem. Inf. Comput. Sci. **34**(2) (1994) 421–427.

[13] K. Balasubramanian, Matching polynomials of fullerene clusters, Chem. Phys. Lett. **201**(1-4) (1994) 306–314.

[14] K. Balasubramanian, K. Khokhani, S.C. Basak, Complex graph matrix representations and characterizations of proteomic maps and chemically induced changes to proteomes, J. Proteome Res. **5**(5) (2006) 1133–1142.

[15] K. Balasubramanian, M. Randić, The characteristic polynomials of structures with pending bonds, Theoret. Chim. Acta **61**(4) (1982) 307–323.

[16] M. Ballerini, N. Cabibbo, R. Candelier, A. Cavagna, E. Cisbani, I. Giardina, V. Lecomte, A. Orlandi, G. Parisi, A. Procaccini, M. Viale, Interaction ruling animal collective behavior depends on topological rather than metric distance: Evidence from a field study, Proceedings of the National Academy of Sciences, **105**(4) (2008) 1232–1237.

[17] S.C. Basak, G.D. Grunwald, B.D. Gute, K. Balasubramanian, D. Opitz, Use of statistical and neural net approaches in predicting toxicity of chemicals, J. Chem. Inf. Comput. Sci. **40**(4) (2000) 885–890.

[18] S.C. Basak, D. Mills, M.M. Mumtaz, K. Balasubramanian, Use of topological indices in predicting aryl hydrocarbon receptor binding potency of dibenzofurans: A hierarchical QSAR approach, Indian J. Chem. **42A**(6) (2003) 1385–1391.

[19] A. Bharali, R. Bora, Computation of some degree based topological indices of silicates (SiO_2) layer, Ann. Pure Appl. Math. **16**(2) (2018) 287–293.

[20] C. Cao, Y. Hua, Topological indices based on vertex, distance, and ring: On the boiling points of paraffins and cycloakanes, J. Chem. Inf. Comput. Sci. **41**(4) (2001) 867–877.

[21] X. Chen, R. Klingeler, M. Kath, A.A.E. Gendy, K. Cendrowski, R.J. Kalenczuk, E. Borowiak-Palen, Magnetic silica nanotubes: synthesis, drug release, and feasibility for magnetic hyperthermia, ACS Appl. Mater. Interfaces **4**(4) (2012) 2303–2309.

[22] M. Črepnjak, N. Tratnik, The Szeged index and the Wiener index of partial cubes with applications to chemical graphs, Appl. Math. Comput. **309** (2017) 324–333.

[23] D. Djoković, Distance preserving subgraphs of hypercubes, J. Combin. Theory Ser. B **14**(3) (1973) 263–267.

[24] E. Estrada, L. Torres, L. Rodríguez, I. Gutman, An atom-bond connectivity index: Modelling the enthalpy of formation of alkanes, Indian J. Chem. **37**A (1998) 849–855.

[25] S. Fajtlowicz, On conjectures of Graffiti-II, Congr. Numer. **60** (1987) 187–197.

[26] F. Farrukh, S. Hafi, R. Farooq, M.R. Farahani, Calculating some topological indices of SiO_2 layer structure, J. Inform. Math. Sci. **8**(3) (2016) 181–187.

[27] F. Farrukh, R. Farooq, M.R. Farahani, On the atom-bond connectivity and geometric-arithmetic indices of SiO_2 layer structure, Mor. J. Chem. **5**(2) (2017) 384–390.

[28] W. Gao, W. Wang, D. Dimitrov, Y. Wang, Nano properties analysis via fourth multiplicative ABC indicator calculating, Arab. J. Chem. (2017) DOI:10.1016/j.arabjc.2017.12.024.

[29] I. Gutman, A formula for the Wiener number of trees and its extension to graphs containing cycles, Graph Theory Notes NY. **27** (1994) 9–15.

[30] I. Gutman, A.R. Ashrafi, The edge version of the Szeged index, Croat. Chem. Acta, **81**(2) (2008) 263–266.

[31] I. Gutman, N. Trinajstić, Graph theory and molecular orbitals. Total φ-electron energy of alternant hydrocarbons, Chem. Phys. Lett. **17**(4) (1972) 535–538.

[32] B. Hemmateenejad, A. Mohajeri, Application of quantum topological molecular similarity descriptors in QSPR study of the O-methylation of substituted phenols, J. Comput. Chem. **29**(2) (2008) 266–274.

[33] P. Horcajada, A. Rámila, J. Pérez Pariente, M. Vallet-Regi, Influence of pore size of MCM-41 matrices on drug delivery rate, Microporous Mesoporous Mater. **68**(1-3) (2004) 105–109.

[34] S. Kasani, P. Zheng, N. Wu, Tailoring optical properties of a large-area plasmonic gold nanoring array pattern, J. Phys. Chem. C **122**(25) (2018) 13443–13449.

[35] P.V. Khadikar, S. Karmarkar, V.K. Agrawal, A novel PI index and its applications to QSPR/QSAR studies, J. Chem. Inf. Comput. Sci. **41**(4) (2001) 934–949.

[36] S. Klavžar, On the canonical metric representation, average distance, and partial Hamming graphs, Eur. J. Comb. **27** (2006) 68–73.

[37] S. Klavžar, I. Gutman, Wiener number of vertex-weighted graphs and a chemical application, Discrete Appl. Math. **80**(1) (1997) 73–81.

[38] S. Klavžar, I. Gutman, B. Mohar, Labeling of benzenoid systems which reflects the vertex-distance relation, J. Chem. Inf. Comput. Sci. **35**(3) (1995) 590–593.

[39] S. Klavžar, A. Lipovec, Partial cubes as subdivision graphs and as generalized Petersen graphs, Discrete Math. **263**(1-3) (2003) 157–165.

[40] S. Klavžar, P. Manuel, M.J. Nadjafi-Arani, R.S. Rajan, C. Grigorious, S. Stephen, Average distance in interconnection networks via reduction theorems for vertex-weighted graphs, Comput. J. **59**(12) (2016) 1900–1910.

[41] S. Klavžar, M.J. Nadjafi-Arani, Wiener index in weighted graphs via unification of Θ^*-classes, Eur. J. Comb. **36** (2014) 71–76.

[42] S. Klavžar, M.J. Nadjafi-Arani, Cut method: update on recent developments and equivalence of independent approaches, Curr. Org. Chem. **19**(4) (2015) 348–358.

[43] M.H. Khalifeh, H. Yousefi-Azari, A.R. Ashrafi, I. Gutman, The edge Szeged index of product graphs, Croat. Chem. Acta. **81**(2) (2008) 277–281.

[44] M.H. Khalifeh, H. Yousefi-Azari, A.R. Ashrafi, S.G. Wagner, Some new results on distance-based graph invariants, Eur. J. Comb. **30**(5) (2009) 1149–1163.

[45] M. Llusar, C. Sanchez, Inorganic and hybrid nanofibrous materials templated with organogelators, Chem. Mater. **20**(3) (2008) 782–820.

[46] A. Mahmiani, O. Khormali, A. Iranmanesh, M. Yousefidaz, The new version of Szeged index, Optoelectron. Adv. Mater.-Rapid Commun. **4**(12) (2010) 2182–2184.

[47] M. Manoharan, M.M. Balakrishnarajan, P. Venuvanalingam, K. Balasubramanian, Topological resonance energy predictions of the stability of fullerene clusters, Chem. Phys. Lett. **222**(1-2) (1994) 95–100.

[48] A. Mohajeri, M.H. Dinpajooh, Structure-toxicity relationship for aliphatic compounds using quantum topological descriptors, J. Mol. Struct. -THEOCHEM **855**(1-3) (2008) 1–5.

[49] A. Mohajeri, P. Manshour, M. Mousaee, A novel topological descriptor based on the expanded Wiener index: applications to QSPR/QSAR studies, Iranian J. Math. Chem. **8**(2) (2017) 107–135.

[50] B. Munoz, A. Rámila, J. Pérez Pariente, I. Diaz, M. Vallet-Regi, MCM-41 organic modification as drug delivery rate regulator, Chem. Mater. **15**(2) (2003) 500–503.

[51] D. Narducci, G. Cerofolini, E. ROMANO, Nanotori of semiconductor material for use in diagnostics and in the anti-tumor therapy and process for the production thereof, https://patents.google.com/patent/WO2012140680A8/en.

[52] T. Parsons-Moss, L.K. Schwaiger, A. Hubaud, Y.J. Hu, H. Tuysuz, P. Yang, K. Balasubramanian, H. Nitsche, Plutonium complexation by phosphonate-functionalized mesoporous silica, 241^{th} ACS National Meeting, Anaheim, CA, United States, 2011.

[53] R. Ramaraj, K. Balasubramanian, Computer generation of matching polynimials of chemical graphs and lattices, J. Comput. Chem. **6**(2) (1985) 122–141.

[54] M. Randić, Characterization of molecular branching, J. Am. Chem Soc. **97**(3) (1975) 6609–6615.

[55] M. Randić, Novel molecular descriptor for structure-property studies, Chem. Phys. Lett. **211** (1993) 478–483.

[56] D.H. Rouvray, R.B. King, Topology in Chemistry: Discrete Mathematics of Molecules, Elsevier, 2002.

[57] H.P. Schultz, Topological organic chemistry. 1. Graph theory and topological indices of alkanes, J. Chem. Inf. Comput. Sci. **29**(3) (1989) 227–228.

[58] N. Tratnik, The edge-Szeged index and the PI index of benzenoid systems in linear time, MATCH Commun. Math. Comput. Chem. **77**(2) (2017) 393–406.

[59] M. Vallet-Regi, A. Rámila, R.P. del Real, J. Pérez Pariente, A new property of MCM-41: drug delivery system, Chem. Mater. **13**(2) (2001) 308–311.

[60] D. Vukičević, B. Furtula, Topological index based on the ratios of geometrical and arithmetical means of end-vertex degrees of edges, J. Math. Chem. **46**(4) (2009) 1369–1376.

[61] H. Wiener, Structural determination of paraffin boiling points, J. Am. Chem. Soc. **69**(1) (1947) 17–20.

[62] P. Winkler, Isometric embeddings in products of complete graphs, Discrete Appl. Math. **7** (1984) 221–225.

[63] H. Yuan, A.L. Parrill, QSAR development to describe HIV-1 integrase inhibition, J. Mol. Struct. -THEOCHEM **529**(1-3) (2000) 273–282.

[64] B. Zhou, N. Trinajstić, On a novel connectivity index, J. Math. Chem. **46**(4) (2009) 1252–1270.

[65] Y. Zhu, J. Shi, W. Shen, X. Dong, J. Feng, M. Ruan, Y. Li, Stimuli-responsive controlled drug release from a hollow mesoporous silica sphere/polyelectrolyte multilayer core-shell structure, Angew. Chem. Int. Ed. Engl. **44**(32) (2005) 5083–5087.